XPAD: pixel detector for material sciences

S. Basolo, J.-F. Berar, N. Boudet, P. Breugnon, B. Caillot, J.-C. Clemens, P. Delpierre, B. Dinkespiler, I. Koudobine, C. Meessen, et al.

XPAD : pixel detector for material sciences

S. Basolo, J.-F. Bérar, N. Boudet, P. Breugnon, B. Caillot, J.-C. Clemens, P. Delpierre, B. Dinkespiler,
I. Koudobine, Ch. Meessen, M. Menouni, Ch. Mouget, P. Pangaud, R. Potheau and E. Vigeolas

Abstract— **Currently available 2D detectors do not make full use of the high flux and high brilliance of third generation synchrotron sources. XPAD prototype, using active pixels, has been developped to fullfill the needs of materials science scattering experiments. At the time, its prototype is build of 8 modules of 8 chips. The threshold calibration of $\approx 4\,10^4$ pixels is discussed. Applications to powder diffraction or SAXS experiments proof that it allows to record high quality data.**

Index Terms— **pixel, detector, synchrotron, diffraction, SAXS.**

I. INTRODUCTION

THE high flux and high brilliance of third generation synchrotron has not been followed by similar progress in detectors. For this reason numerous experiments are still performed using slits and photomultipliers that allow only point detection or using CCD cameras with indirect photon detection when two dimensional detection is required [1]. Hybrid pixel detectors have been developed for high energy physics [2], they present a new opportunity to improve the quality of our measurements.

II. THE XPAD PROJECT

The XPAD photon counting detector, suitable for materials science and small angle scattering experiments similar to those performed on the CRG D2AM beamline, should have the following characteristics : wide dynamic range ($>10^9\,photons/pixel$), saturation rate up to $10^7\,ph/s/pixel$ and a noise lower than $0.1\,ph/s/pixel$. In our detector [3]–[6], incoming photons are converted to an electron cloud in the sensor in which a polarization ensures migration of the charge through the bump to the electronic chip. In each pixel, the electron bunches are then treated by dedicated electronics. By virtue of this wide parallelism, very short reading times can be achieved (less than $1\,ms$).

A. The 8 module prototype

The design of XPAD2 prototypes is based on the first XPAD1 generation : the chips, with pixel size $330 \times 330\,\mu m^2$, were manufactured by AMS with $0.8\,\mu m$ CMOS technology.
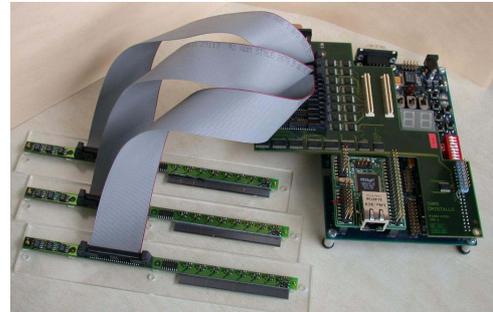
Fig. 1. Three detector modules wired to the acquisition cards.

Owing to the observed wide distribution of the threshold level within XPAD1 chips, parts of the design have been modified to reduce this dispersion. At the same time, the associated electronic was redesigned to fit the project requirements.

The electronics characteristic of the XPAD2 chips have been soon reported [7] then this paper will focuss on the building of a large area detector.

The chips have been bumped to new diodes of $500\,\mu m$ Si thick. Each diode is associated with 8 chips of 24×25 pixels. This unitary assembly appear as an independant module for the output electronic, they are wired to a small PCB card (class 6) which support a few electronic line drivers and voltage regulator (Fig. 1). All the modules are independantly pluged by parallele wiring to the acquisition card, which is based on an Altera Nios developement module and allows direct ethernet communication with the detector.

To build the detector, 8 of these modules have been associated together (Fig. 2). They are tiled as close as possible to each other to reduce shading and dead zones. They have been positioned on a metallic holder with an accuracy of a few microns. The detector size is 200×192 pixels, which gives a surface of about $68 \times 68\,mm^2$.

B. Setting up large array detectors

Even if the dispersion of the threshold level of the pixels has been strongly reduced with the new design of XPAD2 chips, this dispersion has to be taken into account when setting up our detector at the energy of the experiment which is often modified in material sciences to agree with experiment requirement (reciprocal space resolution / completion), sample composition (fluorescence, anomalous effect).

However the increase of the number of pixel in the detector ($\approx 4\,10^4$) leads to develop automatic configuration procedure. At the time, the implemented method uses few steps :

Fig. 2.   The 8 module detector

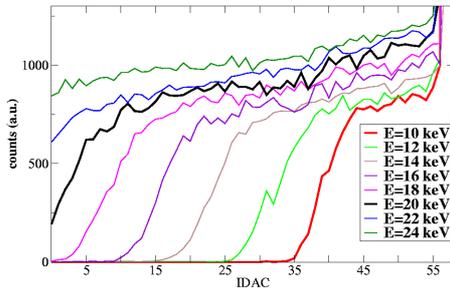Fig. 4.   Scanning a sample in the beam

Fig. 3.   Counts versus pixel threshold at few beam energies.

- All the pixel thresholds are scanned for a few selected beam energies (Fig.3). This is however time consuming.
- Then complementary data are obtained using the "electronic injection mode" : a small defined amount of charges is injected by capacitive coupling.
- Knowing then these characteristics. The setup of each chip at a given energy E can be defined as selecting the value of the chip common threshold level for which most of the pixels can be fine tuned.

In order to obtain accute values of the injection capacitance and therefore to extract reasonable values from injection scans, the measurements using a X-ray beam require monochromaticity and count values in each pixel to be high avoiding poissonian noise. Due to the residual dispersion of electrical characteristics and to the accuracy of the fitting procedures, it revealed the difficulties for finding a configuration in which more than 85% can be simultaneously tuned.

However, even if all the pixels are not perfectly set, the XPAD2 detector appears as a usefull tool for recording new data in SAXS and diffraction on a synchrotron beamline.

C. Kinetics usage of XPAD detector

A wide parallelism has been used in all the design to favour real time measurements. On-board memories allow frames for
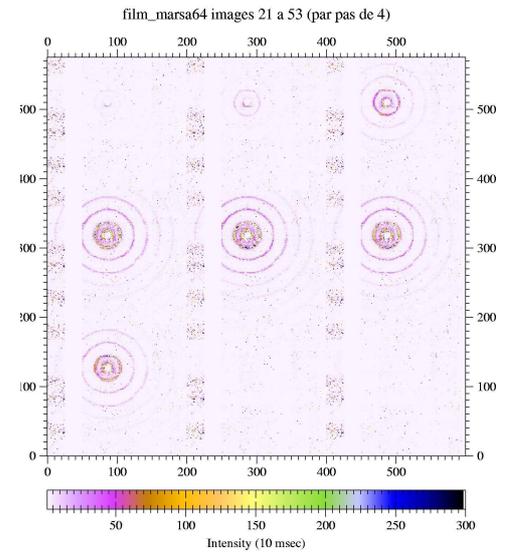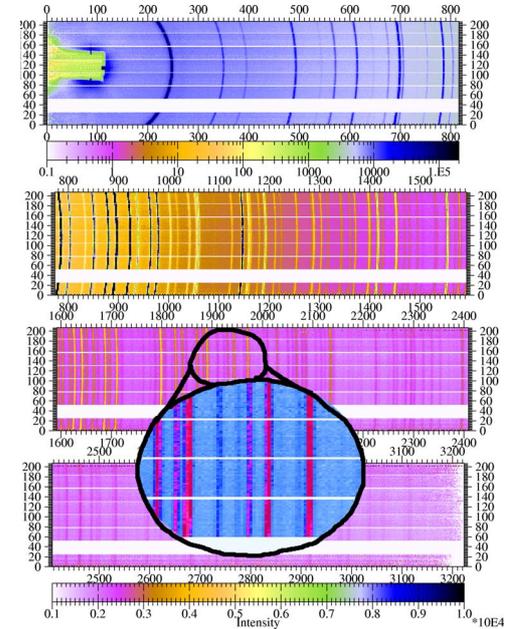

Fig. 5.   Debye Scherrer reconstructed film

these kinetics experiments to be stored : 423 images with less than 10ms exposure or 233 images exposed more than $10\,ms$. The dead time between 2 consecutive images is no more than $2\,ms$. This potentialities are illustrated on Fig. 4 showing the appearence of SAXS diffraction when a moving sample crosses the beam.

III. POWDER DIFFRACTION AND SAXS EXPERIMENT

A. In situ powder diffraction of a CaSrX zeolithe

The powder diffraction is well suited for the study of real catalytic processes : it allows to know accuratly the structure of molecular sieves. However it takes often a long time to record
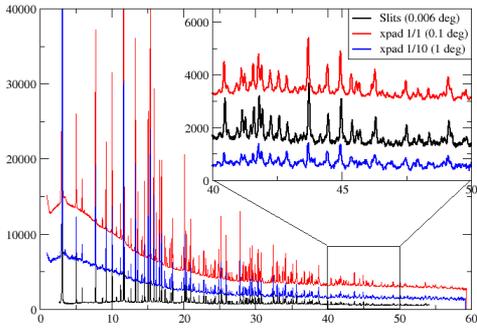
Fig. 6. Scintillator and XPAD powder plot of CaSrX zeolithe.

Fig. 7. Rietveld fit of XPAD experimental data

Fig. 8. XPAD SAXS data: Ag Behenate, polyurethane, water, empty cell.

the diffraction pattern with the needed accuracy, increasing the flux does not allow to reduce strongly this time as an oscillating sample is often needed to reach the statistical orientation average needed by analysis when sample is confined in an in situ reactor with gas pipes. We have compared high quality data recorded with a scintillator counter ($1\,mm$ receiving slit at $1\,m$ from the sample, 60° 2θ at 16 keV) using an angular step of 0.006^o [8]–[10] and XPAD data recorded with the same setting (1m far from sample) with wider angular step but the same exposure time at each step. Data have been processed to build a Debye-Sherrer film represented on Fig. 5 and to obtain the angular plot of the intensity. Using 2θ steps of 0.1^o, the Debye-Sherrer film show information on the whole angular domain. The diffusion at low angle is associated with air scattering and cannot be avoided using 2D detectors. At high angles, measuring weak signal, XPAD data are of very good quality, better than conventional ones (Fig. 6) as it can be seen in the insert where curves have been shifted.

To assess for this quality data have been refined using Rietveld method (Fig. 7). The residual factors reach 4% for Bragg lines and 8% for the whole profile, these values are equivalent to those obtained with conventional data and all refined parameters agree. It appears then possible to record high quality data using XPAD within 1/20 of the time. This reduces the experimental time at each temperature from more than 6 hours to about half an hour, taking into account motions. Data with a wider 2θ step of 1°, are not of the same quality, an oscillation appears in recovering the angular intensity plot. However this is probably due to analysis by software as these oscillations do not appear on raw images.

B. SAXS

Few standard samples have been recorded both using the XPAD detector and a CCD camera (PI-SCX-1300, Roper Scientific (EEG 1340x1300, $50\mu m$ pixel size, dark corrected)) on the D2am SAXS camera using the same setup : detectors have just been exchanged. To reach the needed quality of the images shown on Fig. 8, data have been recorded at few detector positions. Then images have been reconstructed, note that one module has not been recorded due to a diode leakage. The radial distributions have been extracted and they compared
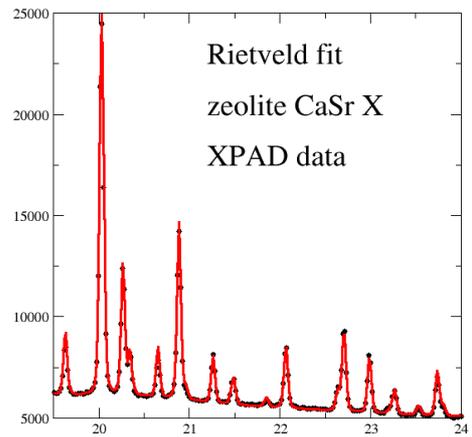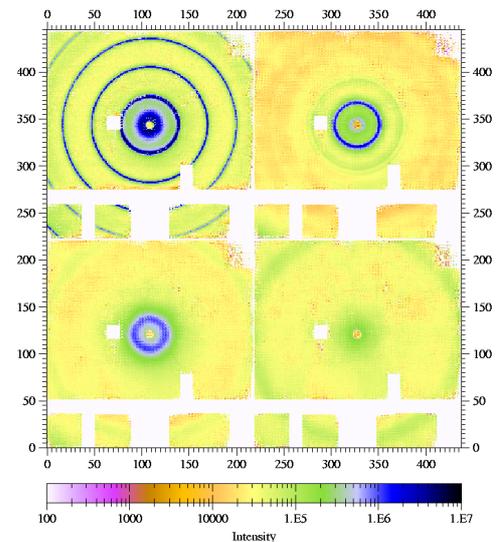
to the CCD ones on Fig. 9. With the CCD all curves tend to the same limit at high Q. It is also difficult to distinguish the weak diffusion of water from those of an empty cell on nearly all the Q range. Using the XPAD, all curves are well separated. This is mainly due to the direct detection. The indirect detection used in the CCD leads to fluorescence decays and/or long PSF tails, these cause an increase of the low level that became not negligible with weak scatterer but do not appears with strong scatterer like polyurethane. One can notice on the figure that the diffusion of the kapton used for all the cell, the ring at high Q, is evident on the empty cell measured with the XPAD.

IV. FUTURE DEVELOPMENTS

Our goal is to develop a real detector with more than 10^6 pixels. Such a detector will consist of several modules to be tiled together. This step has recently been validated by assembling 8 modules of 8 chips each.

To achieve the number of pixels required in numerous experiments, we have already begun the design of a new chip
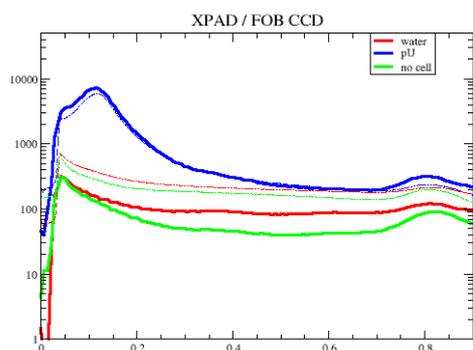
Fig. 9. Radial distributions obtain with XPAD and CCD (dashed)

XPAD3. It will use radiation-hard submicronic technology ($0.25\,\mu m$), which will allow the pixel size to be reduced to $100-150\,\mu m$ with similar or enhanced performance.

ACKNOWLEDGMENT

REFERENCES

[1] L. Brügemann and E. Gerndt *Nucl. Inst. Meth.* vol. A 531 (2004) 292-301.
[2] H. Spieler, *Nucl. Inst. Meth.* vol. A 531 (2004) 1-17.
[3] P. Delpierre, J.-F. Bérar, L. Blanquart, B. Caillot, J.-C. Clemens and C. Mouget, *IEEE Trans. Nucl. Sci.* 48 (2001) 987-991.
[4] P. Delpierre, J.-F. Bérar, L. Blanquart, N. Boudet, P. Breugon, B. Caillot, J.-C. Clemens, C. Mouget, R. Potheau and I. Valin, *IEEE Trans. Nucl. Sci.* vol. 48 (2001) 987-991. 49 (2002) 1709-1711.
[5] J.-F. Bérar, L. Blanquart, N. Boudet, P. Breugon, B. Caillot, J.-C. Clemens, I. Koudobine, P. Delpierre, C. Mouget, R. Potheau and I. Valin, *J. Phys. IV France* vol. 12 (2002) Pr6-385-390.
[6] J.-F. Bérar, L. Blanquart, N. Boudet, P. Breugon, B. Caillot, J.-C. Clemens, P. Delpierre, I. Koudobine, C. Mouget, R. Potheau and I. Valin, *J. Appl. Cryst.* vol. 35 (2002) 471-476.
[7] N. Boudet, J.-F. Bérar, L. Blanquart, P. Breugon, B. Caillot, J.-C. Clemens, I. Koudobine, P. Delpierre, C. Mouget, R. Potheau and I. Valin, *Nucl. Inst. Meth.* vol. A 510 (2003) 41-44.
[8] H. Palancher, J.L. Hodeau, C. Pichon, J.F. Brar, J. Lynch, J. Rodriguez-Carvajal and B. Rebours *Submitted in Angew. Chem. Int. Ed.* 2004
[9] H. Palancher, C. Pichon, B. Rebours, J.L. Hodeau, J. Lynch , J. F. Brar, S. Prevot, G. Conan and C. Bouchard *Submitted in J. Appl. Cryst.* 2004
[10] H. Palancher, C. Pichon, J.L. Hodeau, J.F. Brar, J. Lynch, B. Rebours and J.Rodriguez-Carvajal *Submitted in Zeit. Krist.* 2004